



Minerva Access is the Institutional Repository of The University of Melbourne

Author/s:

Lim, CS;Sozzi, V;Littlejohn, M;Yuen, LKW;Warner, N;Betz-Stablein, B;Luciani, F;Revill, PA;Brown, CM

Title:

Quantitative analysis of the splice variants expressed by the major hepatitis B virus genotypes

Date:

2021-01-01

Citation:

Lim, C. S., Sozzi, V., Littlejohn, M., Yuen, L. K. W., Warner, N., Betz-Stablein, B., Luciani, F., Revill, P. A. & Brown, C. M. (2021). Quantitative analysis of the splice variants expressed by the major hepatitis B virus genotypes. *Microbial Genomics*, 7 (1), pp.1-13. <https://doi.org/10.1099/mgen.0.000492>.

Persistent Link:

<https://hdl.handle.net/11343/278252>

License:

[CC BY](#)

# Quantitative analysis of the splice variants expressed by the major hepatitis B virus genotypes

Chun Shen Lim<sup>1</sup>, Vitina Sozzi<sup>2</sup>, Margaret Littlejohn<sup>2</sup>, Lilly K.W. Yuen<sup>2</sup>, Nadia Warner<sup>2</sup>, Brigid Betz-Stablein<sup>3†</sup>, Fabio Luciani<sup>3</sup>, Peter A. Revill<sup>2,4\*,†</sup> and Chris M. Brown<sup>1\*,†</sup>

## Abstract

Hepatitis B virus (HBV) is a major human pathogen that causes liver diseases. The main HBV RNAs are unspliced transcripts that encode the key viral proteins. Recent studies have shown that some of the HBV spliced transcript isoforms are predictive of liver cancer, yet the roles of these spliced transcripts remain elusive. Furthermore, there are nine major HBV genotypes common in different regions of the world, these genotypes may express different spliced transcript isoforms. To systematically study the HBV splice variants, we transfected human hepatoma cells, Huh7, with four HBV genotypes (A2, B2, C2 and D3), followed by deep RNA-sequencing. We found that 13–28% of HBV RNAs were splice variants, which were reproducibly detected across independent biological replicates. These comprised 6 novel and 10 previously identified splice variants. In particular, a novel, singly spliced transcript was detected in genotypes A2 and D3 at high levels. The biological relevance of these splice variants was supported by their identification in HBV-positive liver biopsy and serum samples, and in HBV-infected primary human hepatocytes. Interestingly the levels of HBV splice variants varied across the genotypes, but the spliced pregenomic RNA SP1 and SP9 were the two most abundant splice variants. Counterintuitively, these singly spliced SP1 and SP9 variants had a suboptimal 5' splice site, supporting the idea that splicing of HBV RNAs is tightly controlled by the viral post-transcriptional regulatory RNA element.

## DATA SUMMARY

The raw RNA-sequencing (RNA-seq) libraries for this study have been deposited in the Gene Expression Omnibus (GSE155983). The PacBio circular consensus sequencing reads analysed in this study have been previously published and can be found in the European Nucleotide Archive (PRJEB12450) [1]. The RNA-seq libraries of hepatitis B virus (HBV)-positive biopsy samples of human liver tumours and tissues, and portal vein tumour thrombosis (129, 182 and 92 libraries, respectively), and HBV-infected primary human hepatocytes (83 libraries) and human cultured cells HepaRG (4 libraries) and HepG2-NTCP (11 libraries) were downloaded from the

Sequence Read Archive [2–18] (see the metadata in Table S1, available with the online version of this article).

## INTRODUCTION

Hepatitis B virus (HBV) is a common human pathogen that is a major cause of liver cirrhosis and liver cancer. The genomic DNA of HBV is approximately 3.2 kb, but can be transcribed into the greater than genome length pregenomic RNA (pgRNA), preC RNA (pcRNA) and long X RNA (lxRNA) [19, 20]. The pgRNA encodes the core (C) and polymerase (P) proteins, whereas the pcRNA encodes the pre-core (PC) protein that is subsequently processed into the hepatitis B e

Received 20 August 2020; Accepted 23 November 2020; Published 13 January 2021

**Author affiliations:** <sup>1</sup>Department of Biochemistry, School of Biomedical Sciences, University of Otago, Dunedin, New Zealand; <sup>2</sup>Victorian Infectious Diseases Reference Laboratory, Royal Melbourne Hospital at the Peter Doherty Institute for Infection and Immunity, Melbourne, Victoria, Australia; <sup>3</sup>Systems Medicine, School of Medical Sciences, Faculty of Medicine, University of New South Wales, Sydney, New South Wales, Australia; <sup>4</sup>Department of Microbiology and Immunology, University of Melbourne, Melbourne, Victoria, Australia.

**\*Correspondence:** Chris M. Brown, [chris.brown@otago.ac.nz](mailto:chris.brown@otago.ac.nz); Peter A. Revill, [peter.revill@mh.org.au](mailto:peter.revill@mh.org.au); [previll@unimelb.edu.au](mailto:previll@unimelb.edu.au)

**Keywords:** HBV; pgRNA; shotgun sequencing; transcriptome assembly.

**Abbreviations:** BCP, basal core promoter; CCS, circular consensus sequencing; coSI, completed splicing index; HBV, hepatitis B virus; HCC, hepatocellular carcinoma; pgRNA, pregenomic RNA; PHH, primary human hepatocyte; PRE, post-transcriptional regulatory RNA element; PVTT, portal vein tumour thrombosis; QC, quality control; RNA-seq, RNA sequencing.

**†Present address:** Dermatology Research Centre, Diamantina Institute, University of Queensland, Brisbane, Queensland, Australia.

**†**These authors contributed equally to this work

**Data statement:** All supporting data, code and protocols have been provided within the article or through supplementary data files. Eight supplementary figures and ten supplementary tables are available with the online version of this article.

000492 © 2021 The Authors



This is an open-access article distributed under the terms of the Creative Commons Attribution License. This article was made open access via a Publish and Read agreement between the Microbiology Society and the corresponding author's institution.

antigen (HBeAg). The HBV genome is also transcribed into several subgenomic transcripts, namely the preS1, preS2, S and X mRNAs. The preS1, S2 and S mRNAs encode the three surface (S) structural proteins of the HBV particles and subviral particles (HBsAg). The X mRNA encodes the HBx protein.

Many strains of HBV have arisen from distinct geographical distributions of the world. This is partly due to the long history of virus–host coevolution (over 50000 years) and the lack of proofreading function of the viral reverse transcriptase [21–23]. These strains were grouped into nine major genotypes (A to I) and putative J, and about 30 sub-genotypes [23, 24]. There are marked differences in replication phenotype and disease natural history across HBV genotypes [25, 26], yet the pathogenicity of different HBV genotypes and their implications for treatment are still not fully understood. For example, it is possible that severe liver injury caused by genotype C is related to its high replication capacity [27] and/or its more frequent mutations at the basal core promoter (BCP) and pre-core regions [28, 29].

In addition, different HBV genotypes may produce distinct spliced transcript isoforms whose precise roles are largely unknown [30–33]. At least 18 spliced transcripts of pgRNA [1, 33–44] and 4 spliced transcripts of preS2/S [45, 46] were identified in various sources including liver, serum and transfected cells. Interestingly, a recent study showed that HBV RNA splicing is more efficient in human hepatoma cells than other tested cell types [33]. Furthermore, spliced pgRNA SP1 is the most commonly detected [35, 36, 38, 40, 47–50], although SP3 and SP9 have also been commonly observed in some studies [1, 32, 33]. These abundant HBV splice variants were previously shown to produce duplex linear DNA and apparent ssDNA species, but rarely relaxed circular DNA [41]. However, their roles in the normal viral life cycle are still unclear.

Notably, HBV splice variants can be encapsidated to form defective viral particles, with replication and envelopment requiring polymerase and envelope proteins supplied *in trans* by wild-type HBV [37, 39, 40, 51]. The SP1 transcript also encodes the hepatitis B spliced protein (HBSP) [47], as well as a truncated (by one amino acid) PC p22 protein that has been shown to inhibit wild-type HBV replication by interfering with wild-type capsid assembly [52]. The HBSP is a fusion product of the first 46 amino acid residues of the P protein and 47 amino acid residues from a distinct reading frame. A recent breakthrough study showed that HBSP could reduce liver inflammation *in vivo* [50]. Three other splice variants that have coding potential are SP7, SP10 and SP13. SP7 encodes the hepatitis B doubly spliced protein (HBDSP), a putative pleiotropic activator, which has been shown to increase replication of wild-type HBV in co-transfection cell culture experiments [53]. SP13 encodes the polymerase-surface fusion protein (P-S FP), a structural protein that could substitute the large HBV surface protein [54]. This fusion protein could inhibit HBV replication and may play a role in persistent infection. Interestingly, SP10

### Impact Statement

Hepatitis B virus (HBV) infection affects over 257 million people worldwide. HBV is a major cause of liver diseases, including cancer, and there is no cure. Although not critical for HBV replication, some HBV RNAs are spliced and the abundant splice variants have been found previously to be associated with liver cancer. The role of these HBV splice variants is still poorly understood. HBV exists as nine genotypes worldwide with marked differences in replicative capacity and disease sequelae. Whether HBV splice variants vary for the different genotypes is yet to be investigated in depth. Here, we sequenced RNAs from four major HBV genotypes using a cell culture system. We found 6 new and 10 previously known splice variants across these genotypes. Some novel HBV splice variants were present at high levels not only in our cell culture system, but also in HBV-positive liver biopsy samples and HBV-infected primary human cells, suggesting they could be functionally important.

could also act as a functional RNA that reduces wild-type HBV replication through interaction with the TATA box binding protein [55].

An increasing number of studies have shown that the HBV splice variants are associated with the development and recurrence of hepatocellular carcinoma (HCC) [49, 56, 57], and poor response to interferon treatment [43]. Therefore, we aimed to utilize RNA-sequencing (RNA-seq) on cells that had been transfected with replication-competent clones of different HBV genotypes to (i) quantify the composition of splice variants at the RNA level, (ii) investigate the effects of sequence variations on splicing efficiency, (iii) determine the usage of splice sites, and (iv) understand the host response to viral replication across the major HBV genotypes A to D.

## METHODS

### Cell culture

Cell culture and transfection experiments were carried out as previously described with the following modifications [25]. Huh7 cells were seeded in six-well plates at partial confluence. After overnight incubation, the cells were transiently transfected with pUC57 constructs harbouring 1.3-mer HBV genomes (genotypes A2, B2, C2 and D3) using FuGENE 6 transfection reagent, according to the manufacturer's instructions (Promega). The generation of plasmids has been previously described and this transient expression system relies on the endogenous promoters of HBV for transcription [25]. The empty pUC57 vector was used as a control. Two independent biological replicates were performed, which included two technical replicates for each treatment.

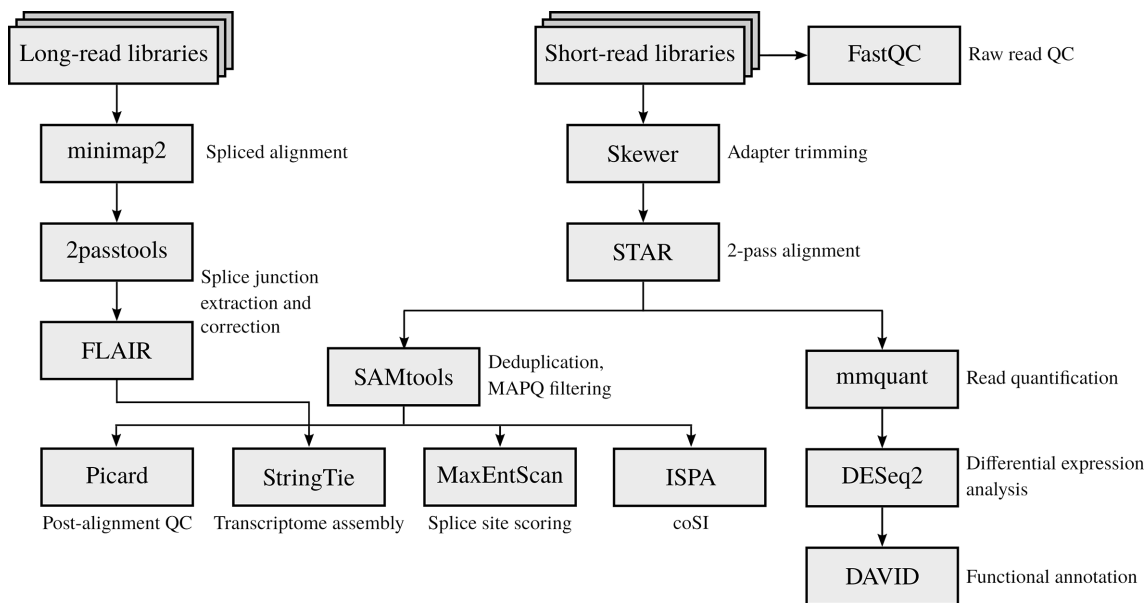


**Fig. 1.** RNA-seq analysis of the HBV and host transcriptomes. QC checking of the paired-end RNA-seq libraries was carried out using FASTQC. Adapter sequences were trimmed from the RNA-seq reads using SKEWER. Trimmed reads were aligned to the human genome and HBV pgRNAs using STAR in 2-pass mode. Duplicated and multi-mapped reads were discarded from the binary alignment map (BAM) files using SAMTOOLS. A post-alignment QC check was performed using PICARD tools. PacBio CCS reads were aligned to the HBV pgRNA using MINIMAP2. HBV splice junctions were extracted and corrected using 2PASSTOOLS and FLAIR, respectively. Reference-based transcriptome assembly and quantification were carried out using STRINGTIE, with a post-processing step focusing on the HBV spliced transcript isoforms. Splice site sequence contexts were scored using MAXENTSCAN. Completeness of RNA splicing was evaluated using IPSA. Reads mapped to human genes were quantified using MMQUANT, followed by differential gene expression analysis using DESEQ2. A list of differentially expressed genes was submitted to the DAVID webserver for functional annotation analysis.

## RNA-seq

Total RNA samples were purified using an RNeasy kit (Qiagen) and submitted to the Otago Genomics and Bioinformatics Facility at the University of Otago (Dunedin, New Zealand) under contract for library construction and sequencing. The libraries were prepared using a TruSeq stranded total RNA sample preparation kit with Ribo-Zero (Illumina) according to the manufacturer's protocol, and sequenced using HiSeq 2500 (Illumina), generating 125 bp paired-end reads (see the RNA-seq analysis workflow in Fig. 1).

## Quality control (QC) of RNA-seq

The fastq files were examined using FASTQC v0.11.5 [58]. Most files passed most of the analysis modules except 'per base sequence content', 'sequence duplication levels' and 'k-mer content', which are common warnings for Illumina TruSeq reads (FASTQC documentation). However, some fastq files failed at per base sequence quality and per base N content due to decrease of the quality score over position 100. Some fastq files also failed at per tile sequence quality due to loss of quality at random positions and cycles, which is likely due to the overloading of the flow cell. Both of these issues should have minimum impact on downstream analysis, because the regions of poor base calling were soft-clipped during alignment. In addition, only uniquely mapped reads were used for gene counting and transcript assembly.

As a post-alignment QC, the mapping statistics of the non-redundant RNA-seq reads were examined. About 60% of the reads were uniquely mapped reads to the human genome (Table S2). The distribution of aligned reads was then analysed using the CollectRnaSeqMetrics program of PICARD 2.10.2 (<http://broadinstitute.github.io/picard>). Over 55 and 27% of the bases of these reads were mapped to the coding sequences (CDS) and untranslated regions (UTRs), respectively (Table S3). Only 10% or lower of the bases of the sequencing reads were aligned to intronic or intergenic regions. These metrics are comparable with previous findings [59], indicating that our RNA-seq libraries are reliable.

## Sequence alignment

Adapter sequences were trimmed from RNA-seq reads using SKEWER v0.2.2 [60]. To detect novel splice junctions, RNA-seq reads were aligned to the human genome and HBV pgRNAs using STAR v2.7.6a in 2-pass mode [61]. Duplicated reads were removed and uniquely mapped reads were retained using SAMTOOLS v1.2 [62] or PICARD MarkDuplicates.

The PacBio circular consensus sequencing (CCS) reads of the whole-genome sequencing of HBV were downloaded from the European Nucleotide Archive (PRJEB12450). This dataset was previously generated from the liver explant and post-transplant blood specimens of a patient with

chronic HBV infection in a longitudinal study [1]. The CCS reads were aligned to a pgRNA sequence (HBV genotype D, GenBank accession no. X02496.1) using MINIMAP v2.17 in splice mode [63]. Splice junctions were extracted and corrected using 2PASSTOOLS and FLAIR, respectively [64, 65]. The BED output file was converted into genotype-specific GTF annotation files using UCSC KENTUTILS [66].

### HBV genotyping

HBV genomic sequence alignment was downloaded from HBVdb [67]. The genomic sequences were converted into pgRNA sequences, split by genotype (A to H), and realigned using MUSCLE v3.7 [68]. A profile hidden Markov model (HMM) was built for each genotype using the hmmbuild program of HMMER v3.3.1 [69]. The RNA-seq reads mapped to HBV were searched against the profile HMMs using NHMMER [70]. A median bit score was calculated for hits to each genotype, in which the highest-scoring genotype was assigned to the RNA-seq BioSamples. As validation, this method accurately predicted the HBV genotypes of the transfected Huh7 and infected primary human hepatocyte (PHH) samples.

### Transcriptome assembly

HBV splice variants were detected using STRINGTIE v1.3.3b [71] and guided by the HBV transcript annotation obtained from the above long-read analysis. Only the splice variants supported by a minimum splice junction coverage of two and with complete, exact match intron chains across independent biological replicates were reported.

Annotations of the spliced transcript isoforms were merged by biological replicates using GTFMERGE (<https://github.com/Kingsford-Group/rnaseqtools>) and GFFCOMPARE [72]. Only the assembled spliced transcripts that were found in both biological replicates were reported (intersection of complete, exact match intron chain). After merging the BAM (binary alignment map) files by biological replicates using SAMTOOLS, a spliced graph of HBV transcripts was plotted using GVIZ v1.32.0 and GENOMICFEATURES v1.40.1 [73, 74]. Transcription start sites were annotated according to a published cap analysis of gene expression [75].

### Splice site analysis

Splice site sequence contexts were scored using MAXENTSCAN [76]. This tool is a key plugin of the Ensembl Variant Effect Predictor [77] and performed the best in a recent benchmark [78]. Splice site mapping frequencies were parsed from the SJ.out.tab file from STAR. IPSA was used to calculate the completed splicing index (coSI) score of 5' and 3' splice sites (<https://github.com/pervouchine/ipsa>) [79]. WEBLOGO 3.5.0 was used to plot the nucleotide frequencies surrounding the splice sites [80].

### Differential gene expression analysis

To examine the reproducibility of the biological replicates, the uniquely mapped reads were first counted and summarized

at the gene level using MMQUANT v1.3 [81]. The correlation of samples was analysed. The Spearman's correlations between the biological replicates were >0.9, suggesting a good reproducibility (Fig. S1). However, the Spearman's correlations between biological replicates were smaller than those within the same batch (e.g. A2\_rep1 versus A2\_rep2 is 0.938, whereas A2\_rep1 versus B2\_rep1 is 0.996). These results suggest the presence of batch effects, which is likely due to the second biological replicate being performed a year after. This was further examined using principal component analysis (PCA). Indeed, the samples were clustered by batches (Fig. S2).

To resolve the issue of batch effects, read counts were transformed using the vst (variance-stabilizing transformation) function of DESEQ2 [82]. Transformed read counts were examined using the plotPCA function of DESEQ2 before and after correction using the removeBatchEffect function of LIMMA [83]. To take batch effects into account, differential-expression analysis was carried out using batch as a linear term in the DESeqDataSetFromMatrix function. Differentially expressed genes were examined using DAVID functional annotation tools v6.8 [84, 85].

### Statistical analysis

Welch two-sample *t*-tests and permutation tests were performed using the EXACTRANKTESTS R package [86, 87]. Plotting was carried out using GGLOT2, unless otherwise stated [88].

### Code and data availability

Scripts and data for the analysis can be found at [https://github.com/lcscs12345/HBV\\_splicing\\_paper\\_2020](https://github.com/lcscs12345/HBV_splicing_paper_2020).

## RESULTS AND DISCUSSION

### Six of sixteen HBV splice variants detected were novel transcripts

Cells were transfected with four different genotypes and total RNA extracted after 24 h, depleted of rRNAs and deep-sequenced. In addition to the well-established subgenomic and spliced transcripts, this method allowed us to detect spliced transcripts with greater sensitivity. The Huh7 cell transfection system showed that HBV genotypes A to D expressed a large proportion of spliced transcript isoforms. These splice variants represented 13–28% of the HBV transcriptomes detected (Fig. 2a), showing that HBV splicing was common, and found across the genotypes. HBV genotype B2 expressed the highest level of HBV transcripts, followed by A2, C2 and D3 [4812, 5442, 4708 and 3972 TPM (transcripts per kilobase million mapped reads), respectively; see also Fig. S3, Table S4 for read counts].

A total of 16 splice variants were consistently detected across two independent biological replicates, in which 6 of them were novel (Figs 2b, 3 and S4, labelled pSP). In particular, a novel, singly spliced RNA (pSP12) was expressed at high levels in the genotypes A2 and D3 (4.5–6.2% of HBV splice variants).

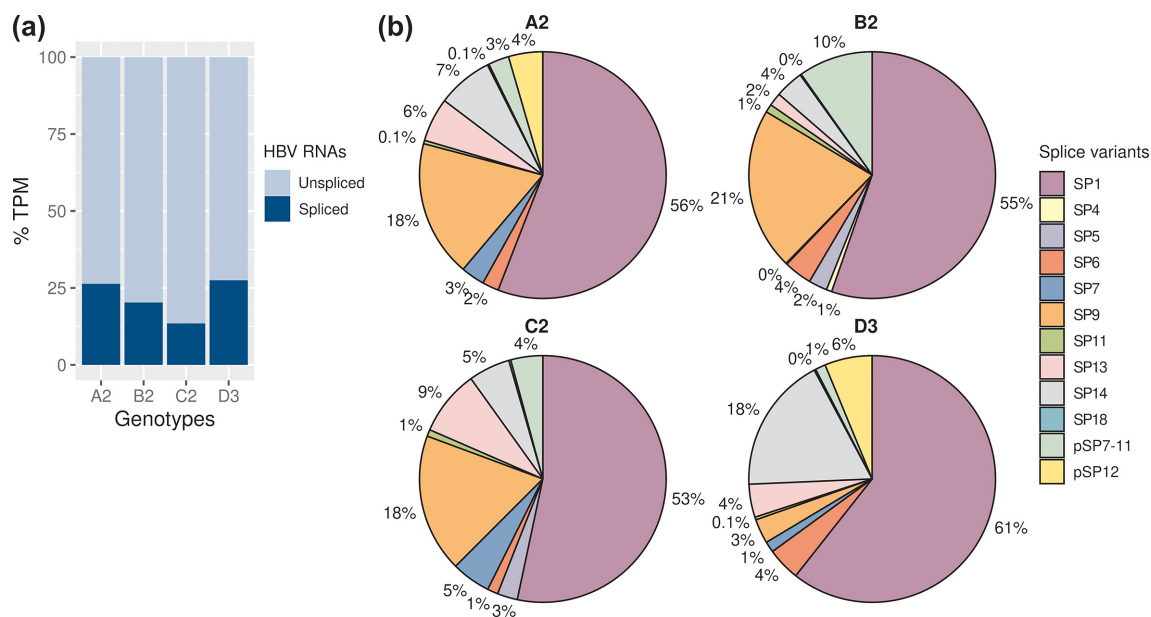


**Fig. 2.** HBV genotypes expressed a wide variety of spliced transcript isoforms. (a) Proportions of the spliced transcripts in HBV RNAs. Only the spliced transcripts present in both biological replicates are shown. (b) Relative abundance of the HBV splice variants in genotypes A to D. See also Tables S4 and S5.

Previously reported splice variants SP1, 4, 5, 6, 7, 9, 11, 13, 14 and 18 were detected in the HBV genotypes [30, 33, 41, 43, 55] (Figs 2–4, Table S5). Notably, these known splice variants were consistently detected in all four genotypes, except for SP4 and SP5. As expected, SP1 was the major spliced transcript detected, ranging from 7.2 to 17% of the HBV transcriptomes, which is in agreement with previous findings [30, 32, 89]. SP9 was the second most abundant spliced transcript, ranging from 0.9 to 4.7% of the HBV transcriptomes. We also detected high but variable levels of SP13 and SP14 across the genotypes, whereas SP6 was the next most abundant.

### Condition- and genotype-specific expression profiles of splice variants in human liver and infected primary cells

To explore the biological relevance of these splice variants identified in a transfection model, we analysed 501 publicly available RNA-seq libraries (Table S1). These came from a diverse range of studies from HBV-positive liver biopsy samples, and HBV-infected PHHs, and different cell lines (HepaRG and HepG2-NTCP).

Significantly, most of the splice variants detected in Huh7 cells were detected in the biopsy samples and PHHs (Figs 4, S5 and S6, Table S1). Our analysis showed that the novel (pSP12) and known (SP1, SP6, SP9, SP13 and SP14) splice variants were also expressed at high levels in these clinical samples and PHHs.

Furthermore, liver tumour and portal vein tumour thrombosis (PVTT) (portal vein invasion at advanced-stage cancer) samples expressed lower levels of HBV RNAs than

non-neoplastic tissue samples (Fig. S7, Table S6). This has been observed in independent studies [90–92], suggesting that HBV replication is less active in tumours. Strikingly, tumour samples expressed SP13 at significantly higher proportions of HBV RNAs than other samples except for PVTT (Figs 4 and S5, Wilcoxon rank sum tests, Bonferroni–Holm adjusted  $P$  value <0.05). Notably, SP13 encodes a P-S FP that has been shown to inhibit HBV replication [54].

Interestingly, we observed some genotype-specific expression profiles of splice variants across the different systems (HBV-transfected Huh7 cells, non-neoplastic liver tissue samples and HBV-infected PHHs; Figs 4 and S5). In particular, HBV genotype D expressed pSP12 and SP6 at significantly higher proportions of HBV RNAs than other three genotypes (Wilcoxon rank sum tests, Bonferroni–Holm adjusted  $P$  value <0.05).

Overall, we obtained higher numbers of uniquely mapped reads to HBV in Huh7 cells, followed by PHHs, non-neoplastic tissue, tumour and PVTT samples (Fig. S7, Table S6). The HBV read counts per library were also more reproducible in HBV-transfected Huh7 cells. In contrast, we detected low numbers of HBV reads in HBV-infected HepaRG and HepG2-NTCP cells. However, their median library sizes were a quarter or a third larger than other libraries (Fig. S7, Table S6).

### Sequencing depth has little effect on splice variant detection

To investigate how sequencing depth affects splice variant detection, we analysed the correlation between the number of

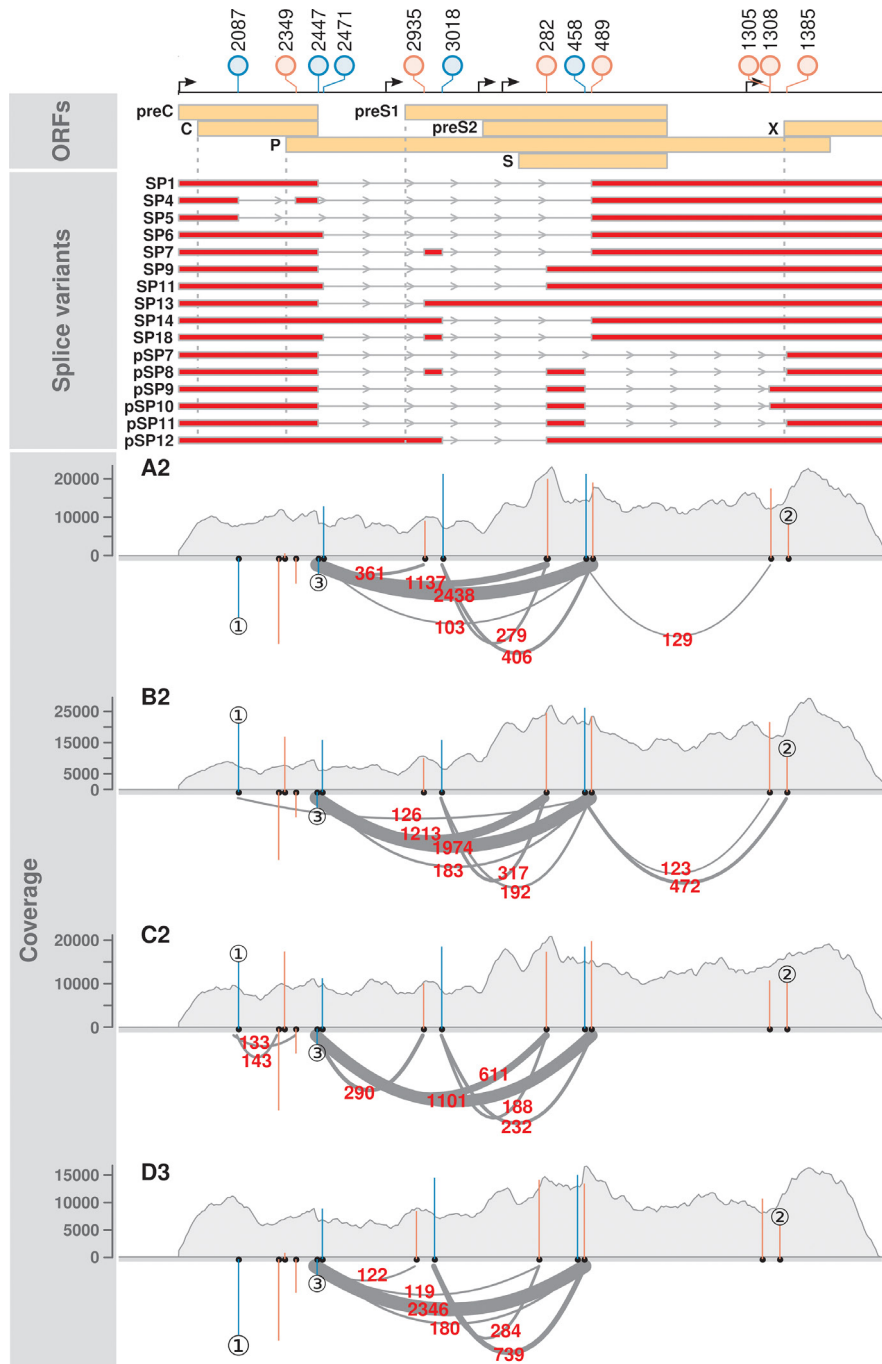


**Fig. 3.** Distinct splicing profiles were observed across the HBV genotypes. The lollipop plot indicates the positions of splice sites relative to the *EcoRI* site of genotype C2. Blue and red colours indicate 5' and 3' splice sites, respectively. SP and pSP denote the known and putative spliced pgRNA transcripts, respectively (splice variants panel). These splice variants were reproducibly detected across the independent biological replicates of HBV-transfected Huh7. Grey dotted lines denote the positions of initiation codons of C, P, preS1 and X reading frames (ORFs panel). Read coverage is shown in grey (coverage panel). Arcs represent RNA-seq reads mapped across the splice junctions (supporting read counts in red colour). Only the splice junctions supported by  $\geq 100$  reads are shown for readability purposes. Blue and red vertical lines indicate the MaxEntScan scores of the 5' and 3' splice sites, respectively (coverage panel). A positive MaxEntScan score predicts a good splice site sequence context, whereas a negative score predicts a poor splice site sequence context. Three main scenarios were observed. ① The presence and absence of spliced reads at position 2087 were predicted by MaxEntScan scores, in which reads were found to map across the 5' splice sites with strong positive scores (B2 and C2), but not those with strong negative scores (A2 and D3). ② Varying spliced read counts could not be explained by similar scores. ③ Most spliced reads were mapped across a weak splice donor site. See also Fig. S4, Table S8.

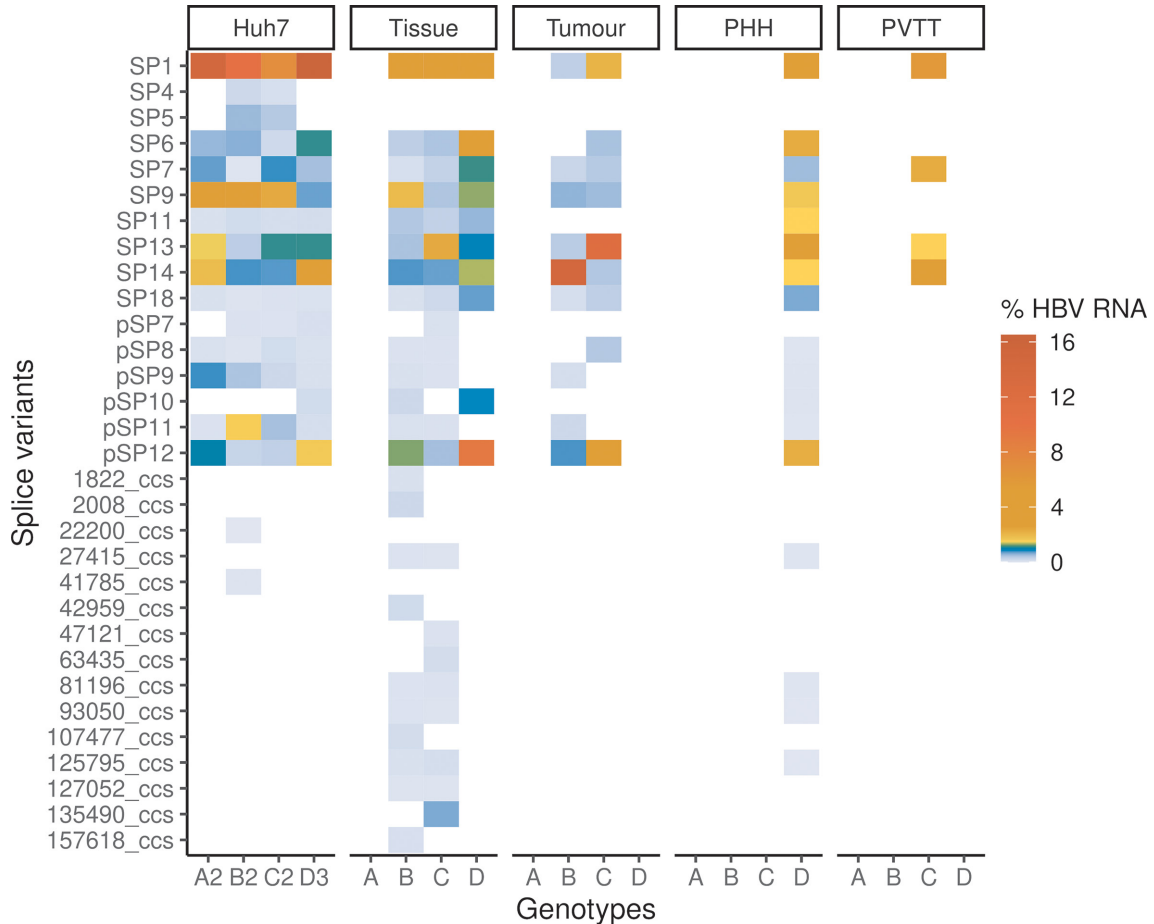


**Fig. 4.** Expression profiles of HBV splice variants in HBV-transfected Huh7 cells, HBV-infected PHHs and biopsy samples. The heatmaps show the mean percentages of HBV RNAs that were spliced. The RNA-seq libraries that had  $\geq 5$  splice variants are shown. The known (SP) and putative (pSP) splice variants were reproducibly detected across the independent biological replicates of HBV-transfected Huh7. Other splice variants are represented with PacBio CCS read names (see Methods). See also Figs S4–S6, Table S1.

unique RNA-seq reads mapped to HBV and library size. Strikingly, we observed weak correlations between the number of uniquely mapped reads (and spliced reads) to HBV and library size (Fig. S7, Kendall's Tau coefficients of 0.20 and 0.13,  $P$  values of  $5.6 \times 10^{-11}$  and  $1.7 \times 10^{-5}$ , respectively). Moreover, HBV spliced reads between biopsy samples could differ by an order of magnitude (Table S6). These results show that splice variant detection differs with genotypes and/or experimental conditions rather than only sequencing depth.

We observed that sequence alignment using a matched HBV genotype is critical in splice variant detection (Fig. S8). A total of 103 of 449 RNA-seq libraries have no uniquely mapped reads to HBV genotype A2 with 11476 reads missing on average. By mapping to the corresponding HBV genotypes, we were able to detect splice variants in 267 of 501 publicly available RNA-seq libraries. Therefore, mapping RNA-seq reads to the HBV reference sequence may not be an appropriate approach and may partly explain the lack of prior reporting. However, most of the reports describing these 501 libraries did not look for splice variants and had other foci.

Taken together, the above findings suggest that Huh7 and PHH systems are more suitable for studying splice variants than clinical samples as: (i) HBV transcription and splicing were more reproducible in Huh7 and PHH systems than other biological materials and systems (Figs S5 and S7, Table S6), (ii) HBV RNAs in clinical samples could be very complex due to the presence of HBV quasispecies (in particular with deletions; Fig. S6), and (iii) the expression of HBV–human chimeric genes as a result of HBV integration [9, 91].

#### Deletions at the X reading frame or BCP detected in HBV-positive biopsy samples

Deletions and splicing in the X reading frame have been reported previously [31, 45, 46, 93–95]. A careful examination of the RNA variants detected revealed three distinct deletions at the X reading frame or BCP (Fig. S6, Table S7). The deletion at positions 1757–1777 (20 bases) was the most common, which was detected in 6 of 41 HCC patients from two continents [7, 9]. In contrast, the 1719–1740 and 1749–1770 deletions (21 bases) were each detected in only one HCC patient.

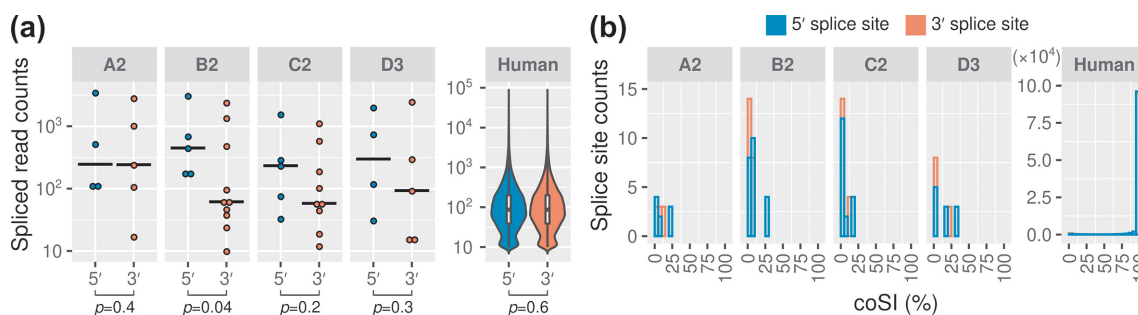


**Fig. 5.** HBV 5' splice sites are more likely to be spliced than 3' splice sites. (a) More spliced reads were mapped across the 5' splice sites of HBV than 3' splice sites. Similar results were obtained from Welch two-sample *t*-test (one-sided) and permutation test (e.g. *P* values of 0.04 and 0.06 were obtained for genotype B2, respectively). Solid black lines indicate median values. (b) Completeness of splicing at the 5' and 3' splice sites. Only the splice sites supported by  $\geq 10$  reads were included for comparison.

Two of these variants 1719–1740 and 1757–1777 co-locate with canonical splice sites (GU-AG), although they could be attributed to DNA mutations.

Interestingly, two of these deletions (1757–1777 and 1749–1770) were previously identified in the DNA of HBV quasispecies (Table S7) [93–95]. No matches were found for the 1719–1740 deletion, this in-frame deletion is novel. These findings suggest that aberrant splicing may be an avenue for the generation of quasispecies, in which the aberrantly spliced pgRNAs may be packaged and reversed transcribed. Moreover, deletions at X/BCP may contribute to the development of HCC [23, 96].

### Sequence variations surrounding the HBV splice sites affect splicing efficiency

We next investigated whether the sequence contexts of splice sites would be predicted to contribute to the different types and abundance of splice variants observed across genotypes. MaxEntScan scoring of the HBV splice sites showed that sequence variation was predicted to affect the strength of the splice sites of the different HBV genotypes (Fig. 3, Table S8).

In general, splice sites with weak sequence contexts (negative MaxEntScan scores) were less likely to be used for splicing and vice versa. For example, the splice donor site at position 2087 in genotypes A2 and D3 had poor sequence contexts and spliced reads associated with this site were not detected (see ① in Fig. 3, Table S8). In contrast, the same donor position in genotypes B2 and C3 had strong sequence contexts and were supported by over 100 spliced reads. This indicates that the splicing efficiencies of the HBV RNAs are strongly influenced by the HBV sequence variants surrounding the splice sites. Indeed, SP5 was not detected in the genotypes A2, D3 and a patient, who was a chronic carrier of HBV genotype D.

However, we also observed a discordance between splice site sequence contexts and splice read counts. For example, all the genotypes had similar scores at the splice acceptor position 1385, but the splice read counts were markedly different (see ② in Fig. 3, Table S8). In particular, the most frequently used

5' splice site that was used for SP1 and SP9 had a negative MaxEntScan score (see ③ or position 2447 in Fig. 3, Table S8).

Taken together, these results suggest that the splicing of this splice junction may be controlled by other *cis* regulatory elements, such as the HBV post-transcriptional regulatory RNA element (PRE) [19]. Indeed, deleting a PRE component called the splicing regulatory element-1 (SRE-1) was previously found to inhibit pgRNA splicing and the production of SP1 [89]. Regulation of alternative splicing may play a crucial role in viral–host interactions [97].

### HBV encoded more alternative 3' splice sites than 5' splice sites

A closer examination of the HBV splicing profiles revealed that HBV encoded more alternative 3' splice sites than 5' splice sites (Figs 3, S4 and S6, Table S8). Indeed, a trend was observed for more spliced reads mapped across the 5' splice sites than 3' splice sites, which reached statistical significance for HBV genotype B2 (Fig. 5). In contrast, host RNAs had balanced numbers of 5' and 3' splice sites (53009 and 52998, respectively), as well as the supported read counts (Fig. 5, median read counts of 87 for both the 5' and 3' splice sites).

To quantify the rates of splicing in HBV versus host cell RNAs, we scored the 5' and 3' splice sites using coSI. The 5' splice sites of HBV showed higher coSI scores than 3' splice sites (9% versus 5% on average; see also Fig. 5). In contrast, splicing was 87 and 86% completed at the host 5' and 3' splice sites, respectively. These results showed that the 5' splice sites of HBV tend to be more frequently spliced than 3' splice sites (e.g. see ② in Fig. 3), but were much less efficiently utilized than host splice sites.

To identify the key differences between the HBV and human genomic splice sites, we compared their splice site contexts using the frequencies of the uniquely mapped, spliced reads to estimate the most frequently used splice sites. This approach showed that the nucleotide frequency distributions of human splice sites were similar to previous studies (Fig. 6) [98]. Notably, the most frequently used splice sites differed between

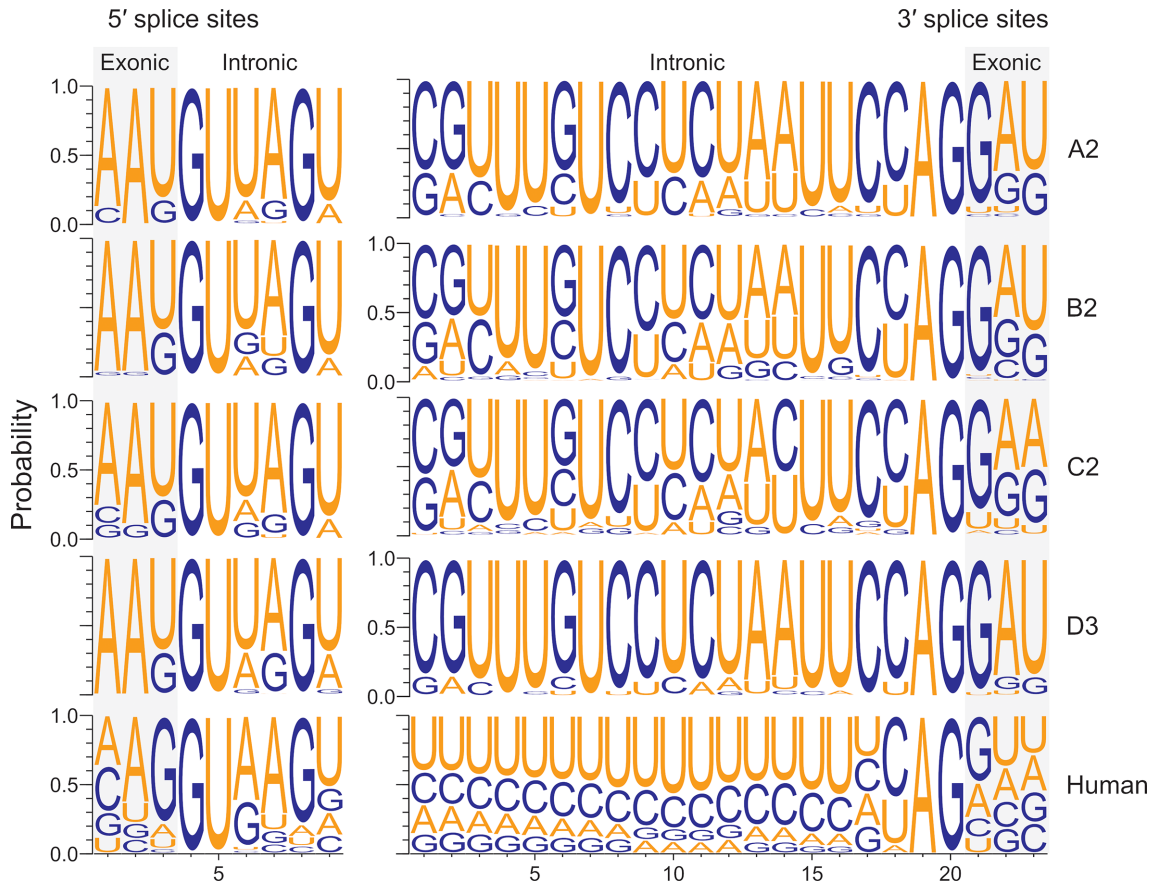


**Fig. 6.** Most frequently used splice sites differed between HBV and the host. The nucleotide frequencies surrounding the splice sites are represented by the spliced reads. Exon boundaries are shaded in grey. Only the splice sites supported by  $\geq 10$  reads were included.

the virus and host, e.g. -1 positions of the splice donor sites (Fig. 6, left panel, U versus G shaded in grey). The differences between the HBV genotypes were marginal, as the spliced reads were predominantly mapped to SP1 and SP9 (Figs 2b and 3).

**HBV replication had little effect on host gene expression in a transfection model**

HBV genomes that were transfected into cells could potentially have significant effects on cellular gene expression, even

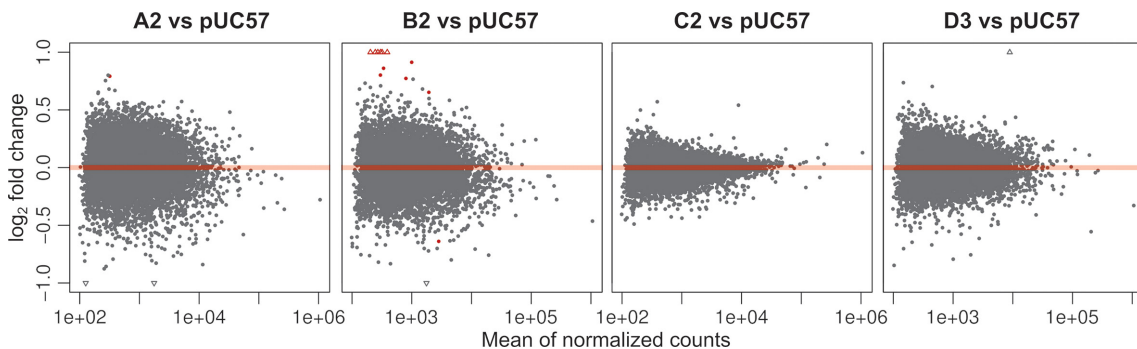


**Fig. 7.** MA plots [log ratio versus mean expression (log scale)] show differential gene expression between the HBV-treated and control samples. Normalized counts indicate the counts divided by the normalization factors (as computed using the DESEQ2 default function). Red points denote the FDR-adjusted  $P$  value of  $< 0.05$ . Unfilled triangles denote the genes that have undergone twofold changes in expression. See also Table S9.

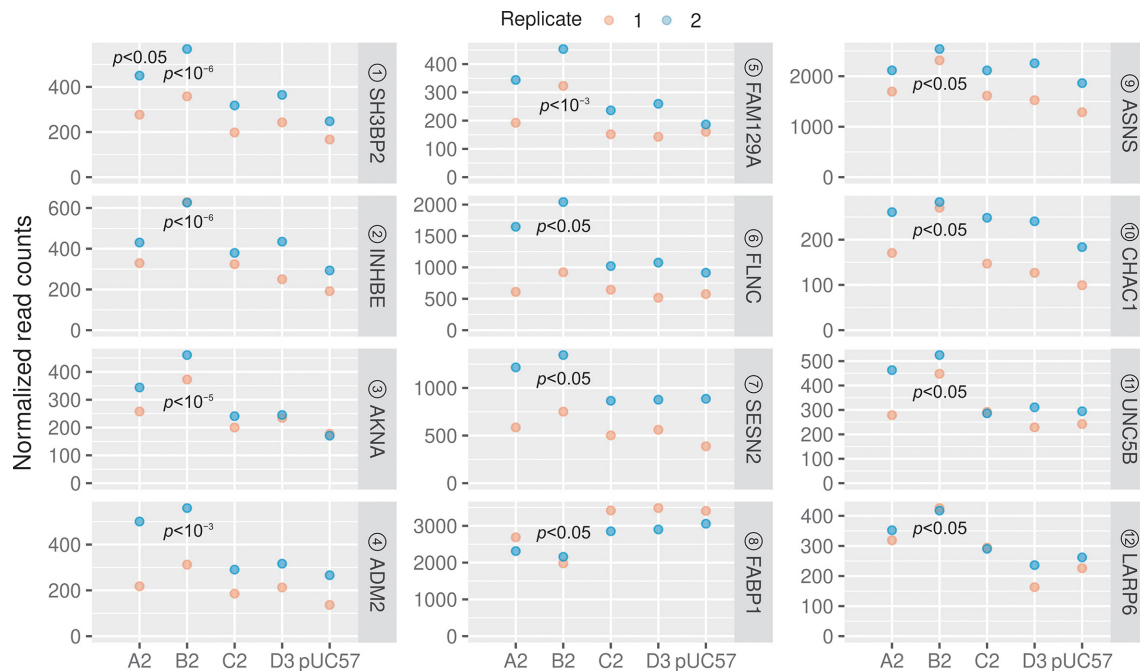


**Fig. 8.** Significantly dysregulated genes in the HBV-treated cells. A total of 12 genes were differentially expressed in the B2-treated sample. Circled numbers denote the ranking based on FDR-adjusted  $P$  values. See also Tables S9 and S10.

after only 24h. To understand the impact of HBV replication on the host, we carried out differential gene expression analysis using DESEQ2 [82]. We found that only 1 and 12 genes were significantly differentially expressed in A2 and B2 treated samples, respectively, compared to the empty plasmid control [Figs 7 (red points) and 8, Table S9, FDR-adjusted  $P$  value  $< 0.05$ ]. Interestingly, both the A2 and B2 genotypes also showed relatively higher levels of HBV transcriptomes than the C2 and D3 genotypes (Fig S3, Tables S4 and S5). The accumulation of HBV transcripts may induce a stress response as the stress-related genes INHBE, FAM129A, SESN2, ASNS and CHAC1 were all upregulated (Fig. 8; see also Table S10 for functional annotation). Indeed, previous studies have also shown that HBV infection could lead to endoplasmic reticulum stress [99–101], including upregulation of INHBE [8, 102]. Interestingly, three significantly upregulated genes (ADM2, AKNA and SH3BP2) were previously shown to correlate with the Ishak fibrosis stage [103]. In particular, ADM2, a gene that is involved in ADORA2B-mediated production of anti-inflammatory cytokines, was also previously found to be differentially expressed in liver tumours [3].

## Concluding remarks

Our study has shed light on the complexity of splicing in four major HBV genotypes in cell lines and patient samples. We identified a number of novel splice variants, as well as previously identified variants, by mapping RNA-seq reads to specific HBV genotypes. Although previous studies have shown that HBV splice variants can be encapsidated, it is expected that the resulting virus particles are defective [1, 37, 39, 40, 51].

While this may apply to the splice variants with a disrupted P reading frame, the deletions or aberrant splicing that we have detected in X/BCP may produce viable quasispecies – their full-length genomic DNAs have been previously sequenced [93–95]. These deletions may be contributing to the development and/or recurrence of HCC [49, 56, 57].

We acknowledge that this study is limited to one member of each of the genotypes, and needs to be expanded to include additional HBV genotypes and subgenotypes. Nonetheless, this study demonstrates that HBV has a large capacity for alternative splicing, likely controlled by *cis*-acting elements such as the PRE [19], which results in high-levels of SP1 and SP9 mRNAs, despite the suboptimal context of the 5' splice site. The role of the SP9 variant in particular needs to be further explored. With up to a quarter of all HBV mRNAs being of spliced origin, the importance of these molecules in the HBV 'life cycle' and pathogenesis requires further investigation.

## Funding information

C. M. B. and C. S. L. were funded by the University of Otago. C. S. L. was a recipient of a Dr Sulaiman Daud 125th Jubilee Postgraduate Scholarship and the Marjorie McCallum travel award. P. A. R., V. S. and M. L. were funded by National Health and Medical Research Council (NHMRC) grant APP1145977.

## Author contributions

C. S. L., C. M. B. and P. A. R. conceived the study. C. S. L. and V. S. conducted the transfection experiments. F. L., B. B.-S., N. W., M. L. and L. Y. generated and provided the PacBio CCS reads. C. S. L. carried out all the bioinformatic and statistical analyses, and wrote the manuscript. C.

M. B. and P. A. R. jointly supervised the study. All authors reviewed and approved the manuscript.

#### Conflicts of interest

The authors declare that there are no conflicts of interest.

#### References

- Betz-Stablein BD, Töpfer A, Littlejohn M, Yuen L, Colledge D et al. Single-molecule sequencing reveals complex genome variation of hepatitis B virus during 15 years of chronic infection following liver transplantation. *J Virol* 2016;90:7171–7183.
- Hou J, Lin L, Zhou W, Wang Z, Ding G et al. Identification of miRNomes in human liver and hepatocellular carcinoma reveals miR-199a/b-3p as therapeutic target for hepatocellular carcinoma. *Cancer Cell* 2011;19:232–243.
- Huang Q, Lin B, Liu H, Ma X, Mo F et al. RNA-Seq analyses generate comprehensive transcriptomic landscape and reveal complex transcript patterns in hepatocellular carcinoma. *PLoS One* 2011;6:e26168.
- Chen J, Li Y, Lai F, Wang Y, Sutter K et al. Functional comparison of IFN- $\alpha$  subtypes reveals potent HBV suppression by a concerted action of IFN- $\alpha$  and - $\gamma$  signaling. *Hepatology* 2020.
- Sato A, Ono C, Tamura T, Mori H, Izumi T et al. Rimona-bant suppresses RNA transcription of hepatitis B virus by inhibiting hepatocyte nuclear factor 4 $\alpha$ . *Microbiol Immunol* 2020;64:345–355.
- Liu PJ, Harris JM, Marchi E, D'Arienzo V, Michler T et al. Hypoxic gene expression in chronic hepatitis B virus infected patients is not observed in state-of-the-art *in vitro* and mouse infection models. *Sci Rep* 2020;10:14101.
- Yang Y, Chen L, Gu J, Zhang H, Yuan J et al. Recurrently deregulated lncRNAs in hepatocellular carcinoma. *Nat Commun* 2017;8:14421.
- Niu C, Livingston CM, Li L, Beran RK, Daffis S et al. The Smc5/6 complex restricts HBV when localized to ND10 without inducing an innate immune response and is counteracted by the HBV X protein shortly after infection. *PLoS One* 2017;12:e0169648.
- Yoo S, Wang W, Wang Q, Fiel MI, Lee E et al. A pilot systematic genomic comparison of recurrence risks of hepatitis B virus-associated hepatocellular carcinoma with low- and high-degree liver fibrosis. *BMC Med* 2017;15:214.
- Hensel KO, Cantner F, Bangert F, Wirth S, Postberg J. Episomal HBV persistence within transcribed host nuclear chromatin compartments involves HBx. *Epigenetics Chromatin* 2018;11:34.
- Niu C, Li L, Daffis S, Lucifora J, Bonnin M et al. Toll-like receptor 7 agonist GS-9620 induces prolonged inhibition of HBV via a type I interferon-dependent mechanism. *J Hepatol* 2018;68:922–931.
- Song M, Sun Y, Tian J, He W, Xu G et al. Silencing retinoid X receptor alpha expression enhances early-stage hepatitis B virus infection in cell cultures. *J Virol* 2018;92:e01771-17.
- Winer BY, Gaska JM, Lipkowitz G, Bram Y, Parekh A et al. Analysis of host responses to hepatitis B and delta viral infections in a micro-scalable hepatic co-culture system. *Hepatology* 2020;71:14–30.
- Moreau P, Cournac A, Palumbo GA, Marbouty M, Mortaza S et al. Tridimensional infiltration of DNA viruses into the host genome shows preferential contact with active chromatin. *Nat Commun* 2018;9:4268.
- De Crignis E, Romal S, Carofiglio F, Moulos P, Versteegen MMA. Human liver organoids; a patient-derived primary model for HBV infection and related hepatocellular carcinoma. *bioRxiv* 2020:568147.
- Li C, Hou Y, Xu J, Zhang A, Liu Z et al. A direct test of selection in cell populations using the diversity in gene expression within tumors. *Mol Biol Evol* 2017;34:1730–1742.
- Liu L, He C, Liu H, Wang G, Lv Z et al. Transcriptomic profiling of long non-coding RNAs in non-virus associated hepatocellular carcinoma. *Cell Biochem Biophys* 2020;78:465–474.
- Wang H, Zhang CZ, Lu S-X, Zhang M-F, Liu L-L et al. A coiled-coil domain containing 50 splice variant is modulated by serine/arginine-rich splicing factor 3 and promotes hepatocellular carcinoma in mice by the Ras signaling pathway. *Hepatology* 2019;69:179–195.
- Lim CS, Brown CM. Hepatitis B virus nuclear export elements: RNA stem-loop  $\alpha$  and  $\beta$ , key parts of the HBV post-transcriptional regulatory element. *RNA Biol* 2016;13:743–747.
- Stadelmayer B, Diederichs A, Chapus F, Rivoire M, Neveu G et al. Full-length 5'RACE identifies all major HBV transcripts in HBV-infected hepatocytes and patient serum. *J Hepatol* 2020;73:40–51.
- Krause-Kyora B, Susat J, Key FM, Kühnert D, Bosse E et al. Neolithic and medieval virus genomes reveal complex evolution of hepatitis B. *eLife* 2018;7:e36666.
- Yuen LKW, Littlejohn M, Duchêne S, Edwards R, Bukulatjpi S et al. Tracing ancient human migrations into Sahul using hepatitis B virus genomes. *Mol Biol Evol* 2019;36:942–954.
- Revill PA, Tu T, Netter HJ, Yuen LKW, Locarnini SA et al. The evolution and clinical impact of hepatitis B virus genome diversity. *Nat Rev Gastroenterol Hepatol* 2020;17:618–634.
- McNaughton AL, Revill PA, Littlejohn M, Matthews PC, Ansari MA. Analysis of genomic-length HBV sequences to determine genotype and subgenotype reference sequences. *J Gen Virol* 2020;101:271–283.
- Sozzi V, Walsh R, Littlejohn M, Colledge D, Jackson K et al. *In vitro* studies show that sequence variability contributes to marked variation in hepatitis B virus replication, protein expression, and function observed across genotypes. *J Virol* 2016;90:10054–10064.
- Kramvis A. Genotypes and genetic variability of hepatitis B virus. *Intervirology* 2014;57:141–150.
- Kao J-H. Molecular epidemiology of hepatitis B virus. *Korean J Intern Med* 2011;26:255–261.
- Kramvis A, Kostaki E-G, Hatzakis A, Paraskevis D. Immunomodulatory function of HBeAg related to short-sighted evolution, transmissibility, and clinical manifestation of hepatitis B virus. *Front Microbiol* 2018;9:2521.
- Chotiayaputta W, Lok ASF. Hepatitis B virus variants. *Nat Rev Gastroenterol Hepatol* 2009;6:453–462.
- Lee GH, Wasser S, Lim SG. Hepatitis B pregenomic RNA splicing – the products, the regulatory mechanisms and its biological significance. *Virus Res* 2008;136:1–7.
- Candotti D, Allain J-P. Biological and clinical significance of hepatitis B virus RNA splicing: an update. *Ann Blood* 2016;2:6.
- Huang C-C, Kuo T-M, Yeh C-T, Hu C, Chen Y-L et al. One single nucleotide difference alters the differential expression of spliced RNAs between HBV genotypes A and D. *Virus Res* 2013;174:18–26.
- Ito N, Nakashima K, Sun S, Ito M, Suzuki T. Cell type diversity in hepatitis B virus RNA splicing and its regulation. *Front Microbiol* 2019;10:207.
- Sommer G, van Bömmel F, Will H. Genotype-specific synthesis and secretion of spliced hepatitis B virus genomes in hepatoma cells. *Virology* 2000;271:371–381.
- Chen PJ, Chen CR, Sung JL, Chen DS. Identification of a doubly spliced viral transcript joining the separated domains for putative protease and reverse transcriptase of hepatitis B virus. *J Virol* 1989;63:4165–4171.
- Su TS, Lai CJ, Huang JL, Lin LH, Yauk YK et al. Hepatitis B virus transcript produced by RNA splicing. *J Virol* 1989;63:4011–4018.
- Terré S, Petit MA, Bréchet C. Defective hepatitis B virus particles are generated by packaging and reverse transcription of spliced viral RNAs *in vivo*. *J Virol* 1991;65:5539–5543.
- Wu HL, Chen PJ, Tu SJ, Lin MH, Lai MY et al. Characterization and genetic analysis of alternatively spliced transcripts of hepatitis B virus in infected human liver tissues and transfected HepG2 cells. *J Virol* 1991;65:1680–1686.

39. Rosmorduc O, Petit MA, Pol S, Capel F, Bortolotti F et al. *In vivo* and *in vitro* expression of defective hepatitis B virus particles generated by spliced hepatitis B virus RNA. *Hepatology* 1995;22:10–19.
40. Günther S, Sommer G, Iwanska A, Will H. Heterogeneity and common features of defective hepatitis B virus genomes derived from spliced pregenomic RNA. *Virology* 1997;238:363–371.
41. Abraham TM, Lewellyn EB, Haines KM, Loeb DD. Characterization of the contribution of spliced RNAs of hepatitis B virus to DNA synthesis in transfected cultures of Huh7 and HepG2 cells. *Virology* 2008;379:30–37.
42. El Chaar M, El Jisr T, Allain J-P. Hepatitis B virus DNA splicing in Lebanese blood donors and genotype A to E strains: implications for hepatitis B virus DNA quantification and infectivity. *J Clin Microbiol* 2012;50:3159–3167.
43. Chen J, Wu M, Wang F, Zhang W, Wang W et al. Hepatitis B virus spliced variants are associated with an impaired response to interferon therapy. *Sci Rep* 2015;5:16459.
44. Lam AM, Ren S, Espiritu C, Kelly M, Lau V et al. Hepatitis B virus capsid assembly modulators, but not nucleoside analogs, inhibit the production of extracellular pregenomic RNA and spliced RNA variants. *Antimicrob Agents Chemother* 2017;61:e00680-17.
45. Hass M, Hannoun C, Kalinina T, Sommer G, Manegold C et al. Functional analysis of hepatitis B virus reactivating in hepatitis B surface antigen-negative individuals. *Hepatology* 2005;42:93–103.
46. Candotti D, Lin CK, Belkhir D, Sakuldamrongpanich T, Biswas S et al. Occult hepatitis B infection in blood donors from South East Asia: molecular characterisation and potential mechanisms of occurrence. *Gut* 2012;61:1744–1753.
47. Soussan P, Tuveri R, Nalpas B, Garreau F, Zavala F et al. The expression of hepatitis B spliced protein (HBSP) encoded by a spliced hepatitis B virus RNA is associated with viral replication and liver fibrosis. *J Hepatol* 2003;38:343–348.
48. Suzuki T, Kajino K, Masui N, Saito I, Miyamura T. Alternative splicing of hepatitis B virus RNAs in HepG2 cells transfected with the viral DNA. *Virology* 1990;179:881–885.
49. Soussan P, Pol J, Garreau F, Schneider V, Le Pendeven C et al. Expression of defective hepatitis B virus particles derived from singly spliced RNA is related to liver disease. *J Infect Dis* 2008;198:218–225.
50. Duriez M, Mandouri Y, Lekbaby B, Wang H, Schnuriger A et al. Alternative splicing of hepatitis B virus: a novel virus/host interaction altering liver immunity. *J Hepatol* 2017;67:687–699.
51. Köck J, Nassal M, Deres K, Blum HE, von Weizsäcker F. Hepatitis B virus nucleocapsids formed by carboxy-terminally mutated core proteins contain spliced viral genomes but lack full-size DNA. *J Virol* 2004;78:13812–13818.
52. Wang Y-L, Liou G-G, Lin C-H, Chen M-L, Kuo T-M et al. The inhibitory effect of the hepatitis B virus singly-spliced RNA-encoded p21.5 protein on HBV nucleocapsid formation. *PLoS One* 2015;10:e0119625.
53. Chen W-N, Chen J-Y, Lin W-S, Lin J-Y, Lin X. Hepatitis B doubly spliced protein, generated by a 2.2 kb doubly spliced hepatitis B virus RNA, is a pleiotropic activator protein mediating its effects via activator protein-1- and CCAAT/enhancer-binding protein-binding sites. *J Gen Virol* 2010;91:2592–2600.
54. Huang HL, Jeng KS, Hu CP, Tsai CH, Lo SJ et al. Identification and characterization of a structural protein of hepatitis B virus: a polymerase and surface fusion protein encoded by a spliced RNA. *Virology* 2000;275:398–410.
55. Tsai K-N, Chong C-L, Chou Y-C, Huang C-C, Wang Y-L et al. Doubly spliced RNA of hepatitis B virus suppresses viral transcription via TATA-binding protein and induces stress granule assembly. *J Virol* 2015;89:11406–11419.
56. Bayliss J, Lim L, Thompson AJV, Desmond P, Angus P et al. Hepatitis B virus splicing is enhanced prior to development of hepatocellular carcinoma. *J Hepatol* 2013;59:1022–1028.
57. Pan M-H, Hu H-H, Mason H, Bayliss J, Littlejohn M et al. Hepatitis B splice variants are strongly associated with and are indeed predictive of hepatocellular carcinoma. *J Hepatol* 2018;68:S474–S475.
58. Andrews S. FastQC: a Quality Control Tool for High Throughput Sequence Data. Cambridge: Babraham Institute; 2016.
59. Sultan M, Amstislavskiy V, Risch T, Schuette M, Dökel S et al. Influence of RNA extraction methods and library selection schemes on RNA-seq data. *BMC Genomics* 2014;15:675.
60. Jiang H, Lei R, Ding S-W, Zhu S. Skewer: a fast and accurate adapter trimmer for next-generation sequencing paired-end reads. *BMC Bioinformatics* 2014;15:182.
61. Dobin A, Davis CA, Schlesinger F, Drenkow J, Zaleski C et al. STAR: ultrafast universal RNA-seq aligner. *Bioinformatics* 2013;29:15–21.
62. Li H, Handsaker B, Wysoker A, Fennell T, Ruan J et al. The Sequence Alignment/Map format and SAMtools. *Bioinformatics* 2009;25:2078–2079.
63. Li H. Minimap2: pairwise alignment for nucleotide sequences. *Bioinformatics* 2018;34:3094–3100.
64. Parker MT, Barton GJ, Simpson GG. Two-pass alignment using machine-learning-filtered splice junctions increases the accuracy of intron detection in long-read RNA sequencing. *bioRxiv* 2020:118679.
65. Tang AD, Soulette CM, van Baren MJ, Hart K, Hrabeta-Robinson E et al. Full-length transcript characterization of SF3B1 mutation in chronic lymphocytic leukemia reveals downregulation of retained introns. *Nat Commun* 2020;11:1438.
66. Lee CM, Barber GP, Casper J, Clawson H, Diekhans M et al. UCSC Genome Browser enters 20th year. *Nucleic Acids Res* 2020;48:D756–D761.
67. Hayer J, Jadeau F, Deléage G, Kay A, Zoulim F et al. HBVdb: a knowledge database for hepatitis B virus. *Nucleic Acids Res* 2013;41:D566–D570.
68. Edgar RC. MUSCLE: multiple sequence alignment with high accuracy and high throughput. *Nucleic Acids Res* 2004;32:1792–1797.
69. Eddy SR. Accelerated profile HMM searches. *PLoS Comput Biol* 2011;7:e1002195.
70. Wheeler TJ, Eddy SR. nhmmer: DNA homology search with profile HMMs. *Bioinformatics* 2013;29:2487–2489.
71. Perteza M, Perteza GM, Antonescu CM, Chang T-C, Mendell JT et al. StringTie enables improved reconstruction of a transcriptome from RNA-seq reads. *Nat Biotechnol* 2015;33:290–295.
72. Perteza G, Perteza M. GFF utilities: GffRead and GffCompare. *F1000Res* 2020;9:304.
73. Hahne F, Ivanek R. Visualizing genomic data using Gviz and Bioconductor. *Methods Mol Biol* 2016;1418:335–351.
74. Lawrence M, Huber W, Pagès H, Aboyoun P, Carlson M et al. Software for computing and annotating genomic ranges. *PLoS Comput Biol* 2013;9:e1003118.
75. Altinel K, Hashimoto K, Wei Y, Neuveut C, Gupta I et al. Single-nucleotide resolution mapping of hepatitis B virus promoters in infected human livers and hepatocellular carcinoma. *J Virol* 2016;90:10811–10822.
76. Yeo G, Burge CB. Maximum entropy modeling of short sequence motifs with applications to RNA splicing signals. *J Comput Biol* 2004;11:377–394.
77. McLaren W, Gil L, Hunt SE, Riat HS, Ritchie GRS et al. The Ensembl variant effect predictor. *Genome Biol* 2016;17:122.
78. Jian X, Boerwinkle E, Liu X. In silico prediction of splice-altering single nucleotide variants in the human genome. *Nucleic Acids Res* 2014;42:13534–13544.
79. Pervouchine DD, Knowles DG, Guigó R. Intron-centric estimation of alternative splicing from RNA-seq data. *Bioinformatics* 2013;29:273–274.
80. Crooks GE, Hon G, Chandonia J-M, Brenner SE. WebLogo: a sequence logo generator. *Genome Res* 2004;14:1188–1190.

81. Zytnicki M. mmquant: how to count multi-mapping reads? *BMC Bioinformatics* 2017;18:411.
82. Love MI, Huber W, Anders S. Moderated estimation of fold change and dispersion for RNA-seq data with DESeq2. *Genome Biol* 2014;15:550.
83. Ritchie ME, Phipson B, Wu D, Hu Y, Law CW et al. Limma powers differential expression analyses for RNA-sequencing and microarray studies. *Nucleic Acids Res* 2015;43:e47.
84. Huang DW, Sherman BT, Lempicki RA. Bioinformatics enrichment tools: paths toward the comprehensive functional analysis of large gene lists. *Nucleic Acids Res* 2009;37:1–13.
85. Huang DW, Sherman BT, Lempicki RA. Systematic and integrative analysis of large gene lists using DAVID bioinformatics resources. *Nat Protoc* 2009;4:44–57.
86. R Core Team. *R: a Language and Environment for Statistical Computing*. Vienna: R Foundation for Statistical Computing; 2020.
87. Hothorn T, Hornik K. exactRankTests: Exact Distributions for Rank and Permutation Tests. Vienna: Comprehensive R Archive Network; 2019.
88. Wickham H. *ggplot2: Elegant Graphics for Data Analysis*. New York: Springer; 2016.
89. Heise T, Sommer G, Reumann K, Meyer I, Will H et al. The hepatitis B virus PRE contains a splicing regulatory element. *Nucleic Acids Res* 2006;34:353–363.
90. Halgand B, Desterke C, Rivière L, Fallot G, Sebah M et al. Hepatitis B virus pregenomic RNA in hepatocellular carcinoma: a nosological and prognostic determinant. *Hepatology* 2018;67:86–96.
91. Jin Y, Lee WY, Toh ST, Tennakoon C, Toh HC et al. Comprehensive analysis of transcriptome profiles in hepatocellular carcinoma. *J Transl Med* 2019;17:273.
92. Marchio A, Cerapio JP, Ruiz E, Cano L, Casavilca S et al. Early-onset liver cancer in South America associates with low hepatitis B virus DNA burden. *Sci Rep* 2018;8:12031.
93. Fang Y, Teng X, Xu W-Z, Li D, Zhao H-W et al. Molecular characterization and functional analysis of occult hepatitis B virus infection in Chinese patients infected with genotype C. *J Med Virol* 2009;81:826–835.
94. Zhou T-C, Li X, Li L, Li X-F, Zhang L et al. Evolution of full-length genomes of HBV quasispecies in sera of patients with a coexistence of HBsAg and anti-HBs antibodies. *Sci Rep* 2017;7:661.
95. Hao R, Xiang K, Peng Y, Hou J, Sun J et al. Naturally occurring deletion/insertion mutations within HBV whole genome sequences in HBeAg-positive chronic hepatitis B patients are correlated with baseline serum HBsAg and HBeAg levels and might predict a shorter interval to HBeAg loss and seroconversion during antiviral treatment. *Infect Genet Evol* 2015;33:261–268.
96. Niller HH, Ay E, Banati F, Demcsák A, Takacs M et al. Wild type HBx and truncated HBx: pleiotropic regulators driving sequential genetic and epigenetic steps of hepatocarcinogenesis and progression of HBV-associated neoplasms. *Rev Med Virol* 2016;26:57–73.
97. Chauhan K, Kalam H, Dutt R, Kumar D. RNA splicing: a new paradigm in host-pathogen interactions. *J Mol Biol* 2019;431:1565–1575.
98. Padgett RA. New connections between splicing and human disease. *Trends Genet* 2012;28:147–154.
99. Li X, Pan E, Zhu J, Xu L, Chen X et al. Cisplatin enhances hepatitis B virus replication and PGC-1 $\alpha$  expression through endoplasmic reticulum stress. *Sci Rep* 2018;8:3496.
100. Liu X, Green RM. Endoplasmic reticulum stress and liver diseases. *Liver Res* 2019;3:55–64.
101. Montalbano R, Honrath B, Wissniowski TT, Elxnat M, Roth S et al. Exogenous hepatitis B virus envelope proteins induce endoplasmic reticulum stress: involvement of cannabinoid axis in liver cancer cells. *Oncotarget* 2016;7:20312–20323.
102. Sasaki R, Kanda T, Nakamura M, Nakamoto S, Haga Y et al. Possible involvement of hepatitis B virus infection of hepatocytes in the attenuation of apoptosis in hepatic stellate cells. *PLoS One* 2016;11:e0146314.
103. Wang Q, Lin L, Yoo S, Wang W, Blank S et al. Impact of non-neoplastic vs intratumoural hepatitis B viral DNA and replication on hepatocellular carcinoma recurrence. *Br J Cancer* 2016;115:841–847.

### Five reasons to publish your next article with a Microbiology Society journal

1. The Microbiology Society is a not-for-profit organization.
2. We offer fast and rigorous peer review – average time to first decision is 4–6 weeks.
3. Our journals have a global readership with subscriptions held in research institutions around the world.
4. 80% of our authors rate our submission process as 'excellent' or 'very good'.
5. Your article will be published on an interactive journal platform with advanced metrics.

Find out more and submit your article at [microbiologyresearch.org](http://microbiologyresearch.org).